

Process Investigation of Tube Expansion by Gas Detonation*

M. Weber¹, M. Hermes², A. Brosius², C. Beerwald², G. Gershteyn³,
H. Olivier¹, M. Kleiner², F.-W. Bach³

¹ Shock Wave Laboratory, Aachen University, Germany

² Institute of Forming Technology and Lightweight Construction, University of Dortmund,
Germany

³ Institute of Material Science, University of Hanover, Germany

Abstract

The present paper deals with the expansion of tubes by direct application of gas detonation waves, i.e. the gas is both pressure medium and energy source. After an introduction to gas detonation forming, measurements of the motion process and the internal pressures are presented. Results of free expansion and of forming into a die are thoroughly studied and compared to the results of quasi-static burst tests and hydroforming. Using pure aluminum Al99.5 and a medium strength alloy AlMgSi1, expansions by 25 % and 20 % respectively are obtained. A simulation delivers details on the deformation process and specially prepared probes of high-speed tension tests give new insight into metallographic material behavior at different strain rates.

Keywords:

Forming, Tube, Shock wave

1 Introduction

Gas detonations have already been applied to sheet metal forming processes and their use in tube forming has also been suggested in the past [17-18], but their potential for the latter purpose and the interactions between the medium, the workpiece, and the tool system have not yet been studied in detail. Besides the well-known advantages of high-speed forming processes, which are higher degrees of formability for various materials and the reduction of press forces due to mass inertia of the tool system [16], the application of gas detonation offers a clean combustion, an easy automation, and less safety regulations compared to the use of solid explosives. Additionally, little need for external apparatuses, high flexibility, and a significant potential for steel forming compared

to electromagnetic forming, have to be mentioned as advantageous attributes. This opens up new possibilities, especially for the expansion of tubes in a die with a great variation of the cross section geometry over the longitudinal axis.

The process of gas detonation and the development of shock waves are theoretically and experimentally explored as far as possible. But the process of expanding tubes by gas detonation causes additional interactions where the constitutive effects influencing the deformation process are still unknown. Therefore, fundamental investigations are necessary in order to offer the possibility for a target-oriented process design in the future. Nowadays, numerical simulation by means of Finite-Element-Simulation (FEA) is an established tool for such tasks. But due to the coupled field problem, containing a mechanical, fluid mechanical, and a chemical part, the simulation and optimization by FEA is not as easy as for conventional forming operations. Therefore, it is important to analyze the process by observing the effects of the detonation on the workpiece with a combined strategy of complementary experimental work and numerical simulation. Thereby, the identification of essential process parameters to achieve a satisfying forming result is a major objective. First results of this fundamental research work are shown in the following.

2 Process principle of gas detonation

The process principle is shown in figure 1. A detonation wave, which is one of the macroscopic manifestations of an explosion, propagates axially through the tube at a stable velocity exceeding multiple sound velocity. Using a pre-compressed stoichiometric mixture of oxygen and hydrogen, the wave speed is about 3,000 m/s, the wave thickness is less than a millimeter, and the pressure immediately behind it exceeds approx. 20 times the initial pressure p_0 of the gas mixture.

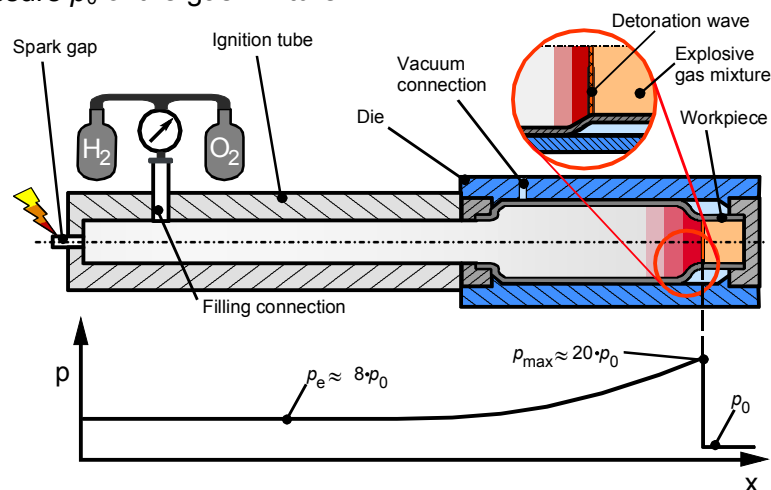


Figure 1: Process principle and experimental set-up

A detonation wave is a joint complex of shock waves and reaction zones, implying shock waves that are strong enough to induce an immediate chemical reaction. The shock compression of the gas is sufficient to cause an instantaneous reaction of the mixture, which quickly leads to a chemical equilibrium. The released heat sustains the wave. The wave is followed by an expansion wave – called Taylor-Expansion – implying a pressure

drop to a value that is approximately 8 times larger than the initial pressure when the gas settles again. The rate of this pressure drop is inversely proportional to the time that has passed since the initiation of the wave. In cylindrical cavities like in tubes this expansion takes about the same time that the wave has already propagated as from its position of initiation. So, the shape of the pressure pulse can be influenced by the length of the whole system, including the ignition tube. The initiation of a detonation wave requires a powerful igniter or a long tube for the transition of the initial deflagration through various states of turbulent combustion. In this work, exploding wires are used for the initiation. When the wave is reflected at the end of a tube it returns as a shock wave without any chemical reaction, leading to an additional pressure jump in the proximity of the reflecting wall. The amplitude of this wave diminishes rapidly, but it reflects several times between the tube ends before its energy is fully dissipated.

3 Experimental set-up and measurement techniques

The set-up for the experimental investigation of free forming processes is shown in figure 2.

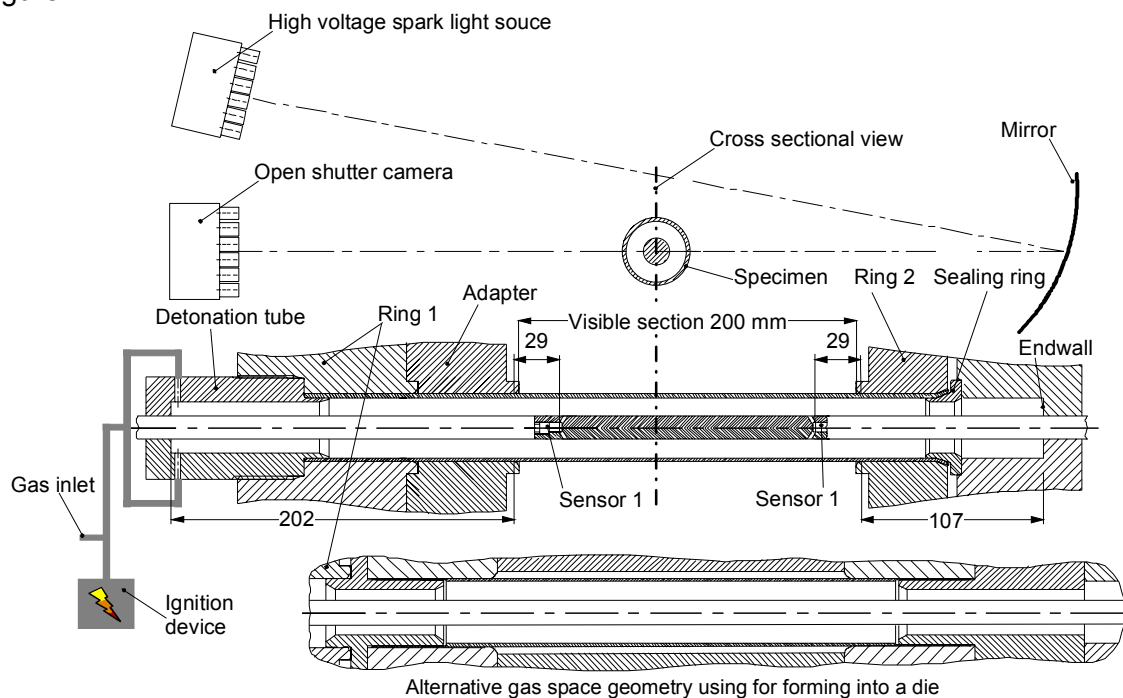


Figure 2: Experimental set-up for the measurement of acting pressure and workpiece deformation in the case of free tube expansion as well as forming into a die

The whole apparatus is filled with gas mixture, which was prepared using mass flow controllers, mixed in a pipe connection, and filled into the evacuated apparatus. The gas detonation is initiated externally by a capacitor discharge through an exploding constantan wire. It enters the detonation tube through the gas inlet and rapidly spreads over the whole cross-section. For an estimation of the pressure pulse width it can be assumed that the wave was initiated at the left end wall. The reason for igniting externally and keeping the detonation tube short was to enable the installation of a coaxial pressure probe that is

fixed in both end walls. It contains two piezo-electric sensors (type Kistler 603B for pressures up to 20 MPa and type Kistler 601H for higher pressures), oriented coaxially and connected to the gasspace by radial bores. The specimen is a tube with 40 mm diameter, 2 mm wall thickness, and with a length of approx. 380 mm. It is internally sealed at both ends. At the right end the tube is clamped while at the left end the tube is capable to deform in axial direction. Ring 2, which consists of two halves, is fixed to Ring 1 by means of rigid frame (not shown in Fig.2), so that the clamping force does not press the specimen axially. The adapter is only a ring to ensure the length of the forming section.

The specimen can be replaced by a thickwalled rigid tube with the same inner diameter to obtain pressure profiles at prevented expanding for comparison. For forming experiments a die (described in Section 6) was installed in the position of the visible section as well as its two neighbouring rings, the sensors being positioned again at 179 and 29 mm upstream of the forming section's end.

The used high speed camera type DRELLO is a 24-axis open shutter system capable of framing frequencies up to 10 MHz, using a conventional still film. The series of high-voltage sparks is triggered by the first pressure sensor. Images were scanned and processed to obtain contour plots of the specimen. As free forming only allows for relatively low initial pressures and forming rates, walls can be installed optionally around the specimen to prevent the motion and, thus, enable the observation of the start phase of faster motion processes. During the operation they are fixed in the above mentioned frame.

3.1 Measurement of acting pressure profile

The pressure records shown in Figure 3 are obtained for free expansion of Al99.5 specimens as well as for prevented deformation at similar initial conditions. Time zero is defined by the original signal at sensor 1, which triggers the camera.

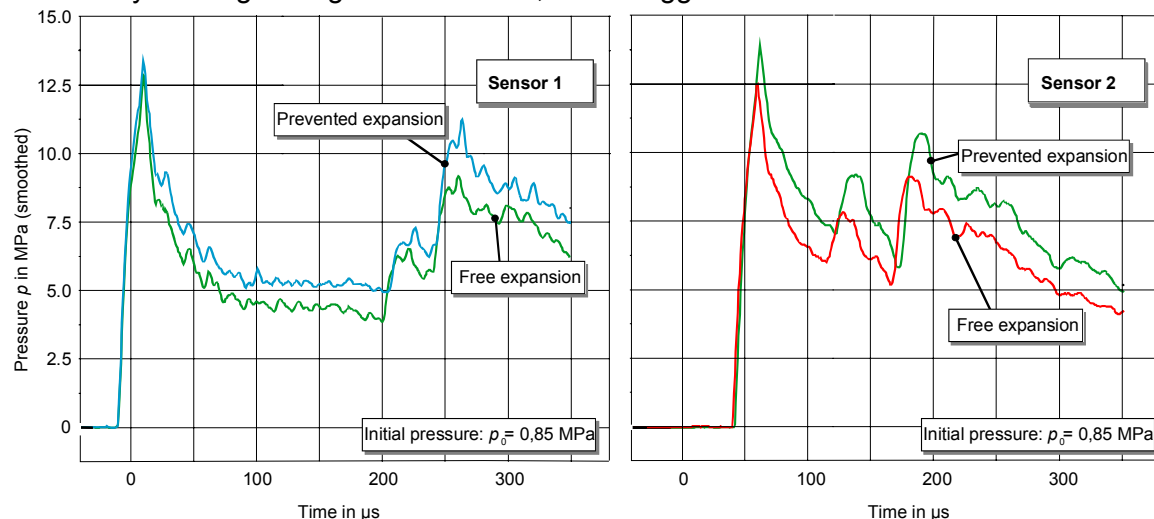


Figure 3: Smoothed pressure records at sensor 1 (left) and 2 (right) from experiments with prevented and free forming of an Al99.5 tube at 0.85 MPa initial pressures. Time zero is defined by the original signal at sensor 1, which triggers the camera

For the prevented deformation experiment the aluminum specimen has been replaced by a thick-walled rigid tube with the same inner diameter. The measured signals have been

smoothed with a half-width of 10 μs to eliminate extreme oscillations. Therefore, the true detonation pressure peak, whose theoretical value is 17 MPa, can not be fully resolved. The second pressure rise is caused by a partial reflection of the detonation wave at the right sealing ring (compare figure 2) and the third one is caused by the reflection at the end wall. Obviously, the expansion of the tube leads to a faster and further pressure drop following the detonation wave because of the increasing volume.

3.2 Measurement of the tube expansion process

Examples of the free expansion process of an Al99.5 specimen are shown in Figure 4. Figures 4a and b show an original high-resolution photograph and the generated contour plots for an initial pressure of 0.85 MPa. The plot that corresponds to the time of 121 μs after passage of the detonation wave at the first sensor almost shows the final shape. In the diagram also the wave front positions at 21 μs and 41 μs are marked. The highest radial velocity of 45 m/s is reached at the end of the free section, shortly before the second sensor shows a second pressure rise (Figure 3), which corresponds to the reflected wave.

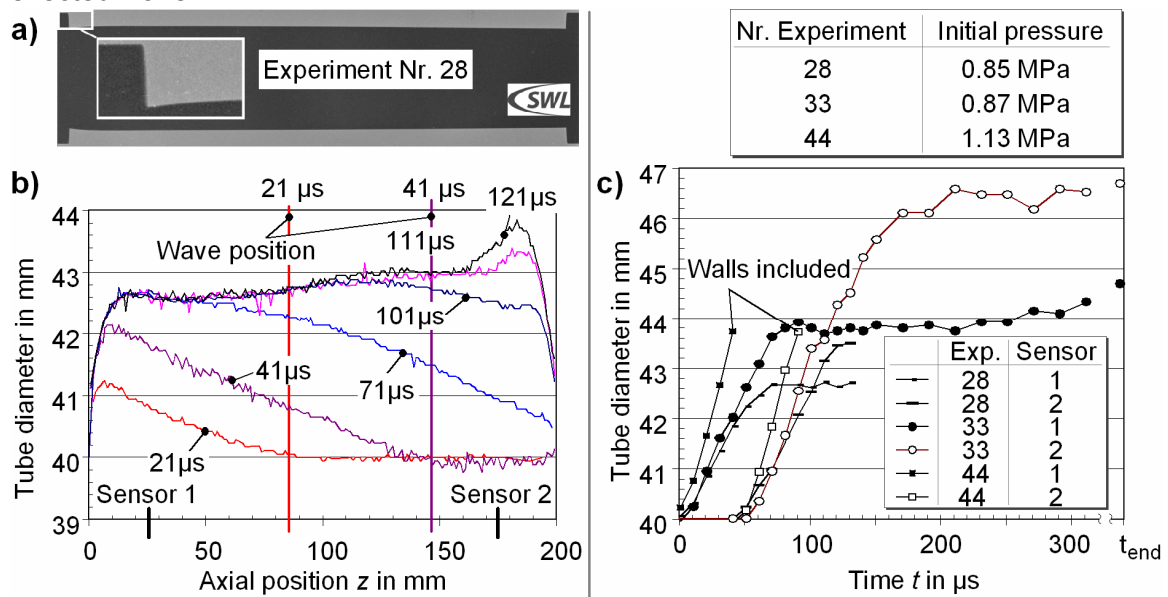


Figure 4: Expansion process of Al99.5 specimens (a) photograph and quad enlargement showing image quality, (b) contour plots and corresponding wave positions, (c) local course of expansion at the axial positions of both pressure sensors

An increase of the pressure to 0.87 MPa led to a much larger expansion, which did not stop within the observation time (see Figure 4c, Exp. 33); the finally reached diameters are given at the right ordinate. This plot shows the maximum achievable diameter of the free expansion of Al99.5 specimens because attempts to increase the initial pressure to 0.9 MPa or more lead to workpiece failure. At the axial position of the first sensor the expansion practically stops at a time of approx. 80 μs . At the second sensor position the expansion is faster. It starts to decelerate when a similar magnitude of expansion as at the first position is reached (at 100 μs), but one frame later it accelerates again due to the currently passing reflected shock wave.

Additionally, Figure 4c shows the start phase of the motion for an initial pressure of 1.13 MPa, where further motion was hindered by the optional supporting walls. A maximum radial velocity of 65 m/s corresponding to a strain rate of 3000 s^{-1} was reached at the position of pressure sensor 2. In these experiments a maximum strain of about 25 % has been achieved. In order to investigate the deformation process numerically, finite element simulations are done, described in the following.

4 Simulation of deformation

As mentioned above, the simulation of this high speed forming process deals with several physical problems which are strongly coupled. Since the consideration of the fluid mechanical field with the usually used Euler formulation will cause numerous numerical problems due to moving boundaries (tube wall) the simulation is uncoupled in a first step. To calculate the pressure time history, a one-dimensional shock tube simulation tool, called KASIMIR developed by the SWL, is used. This tool solves the thermodynamic equilibrium of a shock wave in combination with the chemical reaction using a Riemann solver [3]. The achieved results from this code are applied as time-dependent input in a mechanical simulation using the Finite-Element-Code MSC.MARC in combination with several user-subroutines developed at the IUL. In order to consider the mass inertia effect, the implicit NEWMARK time integration schema is used [3]. To apply the time- and location-dependent force boundary, an ALE-strategy was implemented using a second finite element mesh only for an interpolation of the input data. Fig. 5 shows the two meshes and the relevant boundary conditions.

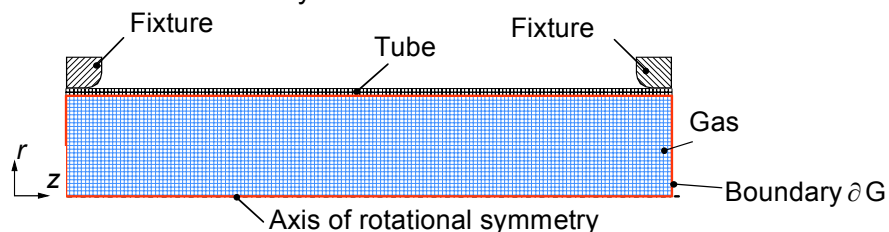


Figure 5: FE-Model using an ALE strategy

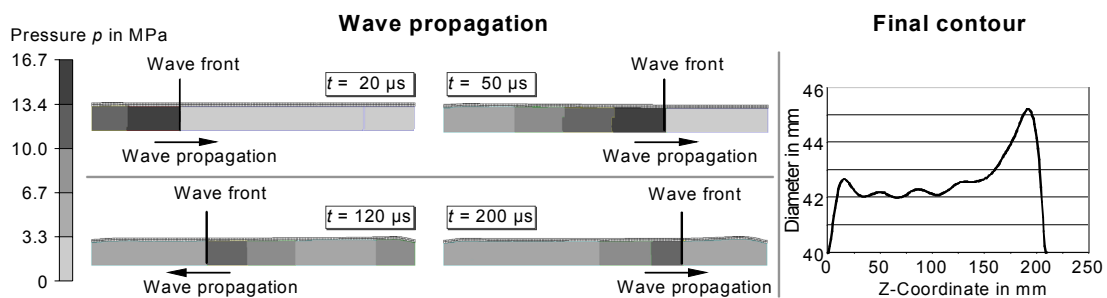


Figure 6: Simulation results of a free forming operation

Fig. 6 shows a result of this simulation strategy by means of a free forming operation. An aluminum tube (Al99.5) with a length of 210 mm, an initial diameter of 40 mm, and a wall thickness of 2 mm was considered. The initial pressure was chosen to $p_0 = 0.85 \text{ MPa}$. Starting with the initiation of the detonation wave, the left end of the tube wall remains for

several microseconds in the initial position until the deformation begins because of its mass inertia. The elastic-plastic deformation process of this initially accelerated tube region is finished when the detonation wave reaches the end of the tube. The time delay between the detonation wave and the movement of the tube wall is also obvious in the measurement data of the free forming operation (Fig. 4, time of 21 μs and 41 μs).

The wave is being reflected at the end of the tube and pressurizes the already accelerated tube again. The final geometry is achieved after the second reflection of the wave. The whole deformation process has a duration of approximately 200 μs , which depends on the starting parameters, e.g. the initial pressure and wave speed, of course. The accordance between this simulation and the experiment can be seen by a comparison of the final contour of the tube (compare Fig. 6b and Fig. 11).

Obviously, the qualitative contour is fitted very well, but from a quantitative point of view large deviations are present. Regarding, this it has to be mentioned that the used simulation strategy is only a first approximation of the real procedure because the pressure drop due to forming and the subsequent volume increase is neglected and the material behavior is unknown. Due to the high strain rate the material behavior differs significantly from the one in quasi-static deformation processes [7, 15]. To overcome this deficit, high speed tensile tests are realized by the Institute of Material Science at the University Hanover (IW) in order to identify the relevant effects.

4.1 Investigation of material behavior

The micro-structural changes as a result of deformation can be described by a multiplicity of structure-relevant parameters. Dislocations and grain boundaries have a substantial influence on the dynamics of the forming process [9, 11]. For example, dislocations within a grain show a different behavior as at or near grain boundaries. These differences are caused by the structure and type of the dislocations [10].

Previous analyses of the dislocation movement and the dislocation density changes as well as the analyses of grain boundary migration took place under thermal activation or at low strain and strain rates. The present results of the conducted analyses can serve as basis for the description of the plastic deformation mechanisms at high strain rates in the finite element simulation. The structural changes were examined using aluminum samples. The processes during plastic deformation are related to different dislocation-drag mechanisms [15]. These are influenced by the following factors:

- thermally activated dislocation movement
- energy of dislocation drag
- impurity viscosity
- phonon viscosity
- electron viscosity.

The first three mechanisms are particularly relevant in static tensile tests with the conventional universal testing machines (tension speed of 2 $\mu\text{m/s}$ to 1,000 mm/min). It is well-known from literature that the mechanism of phonon viscosity is very important at tension speeds of 1 m/s to 1,500 m/s [1].

The processes at the grain boundaries are extraordinarily important as well as the dislocation drag in grains. The grain boundary mobility and its driving strength are the fundamental parameters of the grain boundary slip [13]. The origin of this driving strength has different causes. For most cases the strength results from the differences in the free

energy of the adjacent grains. This difference can be caused by the different surface energies, permeabilities, and disorientations of the adjacent grains or by different dislocation densities on both sides of the grain boundary [6]. By a grain boundary slip the deformation energy stored in the dislocations is set free and the energy of the complete system is minimized. One of the most important procedures for the analysis of the dislocation and the grain boundary structure is the light-microscope etching pit method. Numerous methods were already suggested for the determination of the defect structure in aluminum. At the Institute of Material Sciences a new etching agent as well as a special procedure were developed on the basis of an etching agent, recommended by Barret and Levenson [3]. Using this procedure, the dissolution speed does not depend on the crystallographic orientation so that the etching speed is evenly distributed on specific crystal faces. This procedure can be used for the determination of changes in the defect structure after the deformation of polycrystalline aluminum. A further application is that it is possible to simultaneously corrode grain boundaries, inner-grain dislocation pits, and grain boundary dislocation pits, using the described etching agent in combination with a certain parameter set for electrolytic polishing. The reproducibility of the metallographically determined etching pit density can be determined by comparison with trans-electron-microscopy (TEM) measurements of the dislocation density. The sample material was commercially pure polycrystalline aluminum (99.5%), which was tested in the form of rolled strips of 1 to 4 mm thickness and 70 mm width and of cast slabs of 7 mm thickness and 70 mm width. The tension test samples were prepared from strips and slabs, homogenized for 72 hours at the temperature of 580°C, and were cooled down along with the furnace.

After the tension tests with different test speeds the samples were examined by light-microscopy, parallel to the tension direction (longitudinal axis). The samples for the etching pit method were electrically polished in electrolytes (20% perchloric acid, 10% butylglycol, and 70% ethyl alcohol) with a voltage of 25 V and a flow rate 5 for a duration of 10 s. An etching agent was used for the corrosion (Content: 10% HF, 30% H₂O, 45% HCl and 15% HNO₃). In the following figures examples of the etched microstructure with testing speeds of 2 μm/s (Fig. 7), 1 m/s (Fig. 8), and 6.5 m/s (Fig. 9) are shown. Figure 8a shows that the etching pit arrangement corresponds to a dislocation structure after deformation, whereas the original grain boundaries are marked by pit-free seams. At lower strain rates the dislocation density inside the grain is higher than at increased strain rates, whereas at increased strain rates the dislocations gather at the grain boundaries. (Fig. 8a).

At the test speed of 6.5 m/s (Fig. 9a) particularly many dislocation seams have been formed at or moved to the grain boundaries and the grain boundaries are stretched significantly in tensile direction. The grain boundary slip mechanism and the dislocation movement are both strongly dependent on different strain rates. The changes of the dislocation structure are stronger at increased forming speeds.

The highest tension rate occurs near the fracture zone of the samples and, accordingly, in these areas both aspects of the changed plastic deformation mechanism can be observed best. Here, the following effects can clearly be seen:

- increased dislocation density inside the grains (Fig. 8b)
- increase and redistribution of grain boundary dislocations (Fig. 9b)
- formation of dislocation seams at the grain boundaries (Fig. 9b).

It can be summarized that the analysis shows a strong influence of the strain rate onto the deformation mechanism, causing a different hardening behavior. Therefore, a strain rate dependent material law has to be applied during the finite element simulation in order to improve the quality of simulation. Another important aspect regarding the material behavior during the forming process using gas detonation is the sudden temperature rise. During the process several hundred degrees of Celsius are present at the surface of the deformable structure, but only for a very short duration. To give an advice whether this effect has to be incorporated into the hardening law or not, additional experimental investigations have to be done using an infrared camera measuring system with high-speed option.

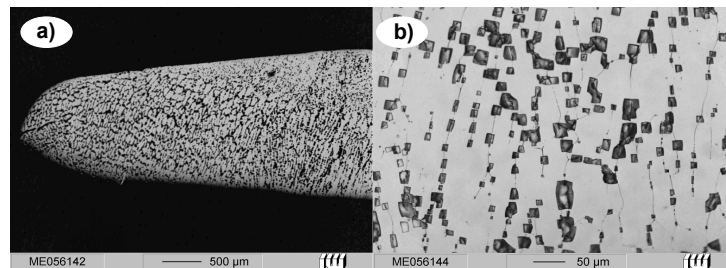


Figure 7: Micrograph of tensile specimen from tensile test with a speed of 2 µm/s

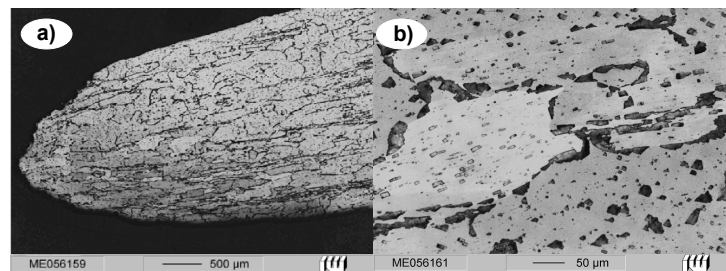


Figure 8: Micrograph of tensile specimen from tensile test with a speed of 1 m/s

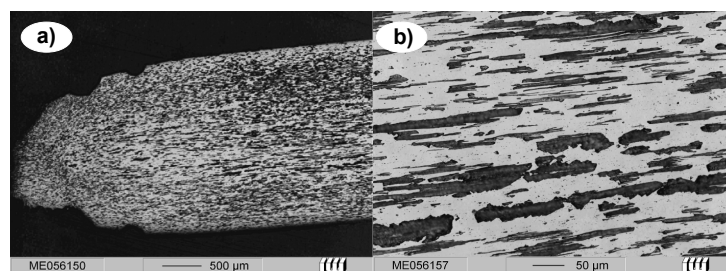


Figure 9: Micrograph of tensile specimen from tensile test with a speed of 6.5 m/s

5 Gas detonation and quasi-static burst tests in die-less forming

Investigations of the free forming process with Al99.5 tubes are necessary to understand the process coherences and to have e.g. the option of optical measurements. The application of the industrial less significant material Al99.5 is interesting for the material investigation to avoid the influence of added alloys.

5.1 Roundness and wall thickness

Before it is possible to use roundness and wall thickness measurements to identify the differences between the two processes the initial state of the specimens is determined. Roundness and wall thickness tests show a good quality of the cross-section geometry of the Al99.5 tube material. The tests were carried out on a CMM and showed that the wall thickness variation is less than 0.2 % and the roundness deviation comes to 0.1 %.

The gas detonation specimens under investigation were made at an initial pressure of 0.85 MPa. The static burst tests were made for the contour measuring at water pressure of approx. 6 MPa to obtain nearly the same diameter as in the measured areas of the gas detonation experiments.

To locate essential properties of the process, e.g. the influence of the higher strain rates on the material, a comparison between expansions by static pressure is essential. A special device was realized at the IUL in order to implement burst tests under static pressure conditions. By the application of a pressure sensor and inductive linear transducers it is possible to indicate the maximum pressure and the according diameter of the expanded tube.

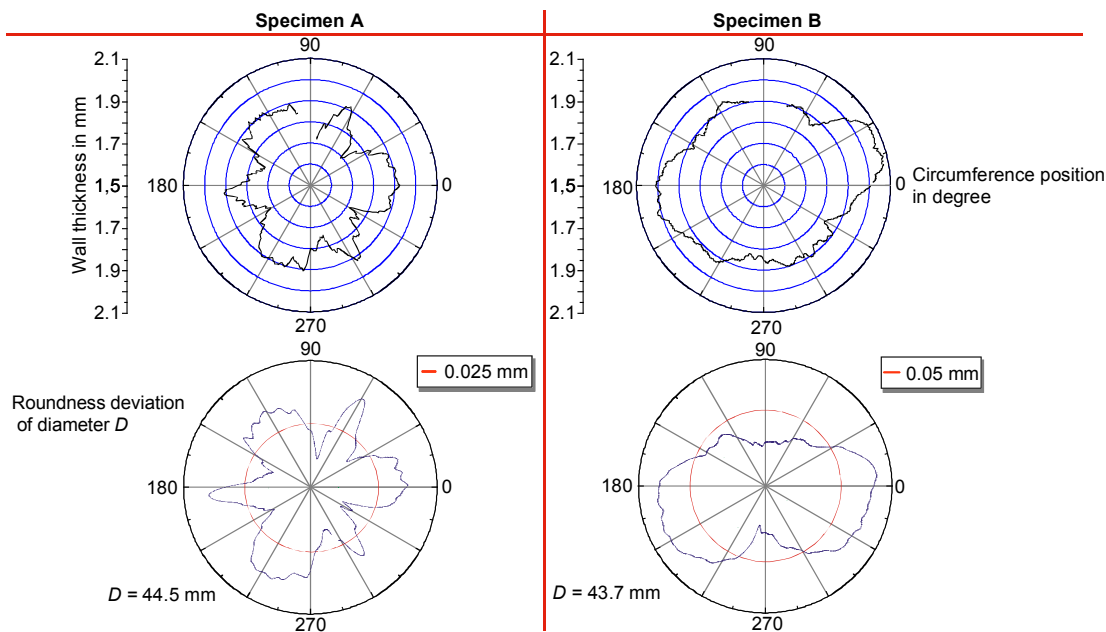


Figure 10: Wall thickness and roundness of the Al99.5 tubes after the gas detonation expansion (specimen A) and water pressure expansion (specimen B)

The specimen A in Figure 10 shows exemplarily the symmetric arrangement of the thicker locations of the wall thickness in the tube formed by gas detonation. They are also present in the roundness diagram because of the same striking peaks on the circumference. This shows that the final deviation from a circular tube cross-section can be partially ascribed to the local thinning of the wall thickness. This means that the good roundness quality of the tubes before the process remains the same. This aspect is caused by the mass inertia forces of the tube walls during the process that stabilize the process in a way that necking is shifted to later deformation states.

The cross-sections of the static burst test specimens (example specimen B) have unsymmetrical and inhomogeneous properties. A reason is the starting necking-in of weak areas along the circumference. The wall thickness of specimen B is, on the average, thicker than of specimen A after the test with static pressure. This is caused by the fact that the material flows in axial direction during expansion. Contrary, the expansion of specimen A is caused by steady material flow out of the wall thickness. The maximum reachable diameter is the same in both processes. Using Al99.5, a diameter of 47 mm die-less is obtainable.

5.2 Lengthwise contour and hardness measurement

The scanning plot in Figure 11 shows the geometry of a specimen made in the gas detonation device without using a die. The maximum at the right end of the curves in the diagram is caused by the reflection of the detonation wave at the end of the device and its interaction with itself, resulting in a sudden pressure rise (see chap. 3).

As expected, the hardness values in Figure 11 rise proportionally to the diameter of the specimen. The hardness at the non-formed ends of the specimen show an average hardness of 22 HV 5. This correlates with the statistic measuring of the bar stock material. The second period of the process that is generated by the reflection of the detonation wave can be seen as a second forming process, which causes additional strain hardening (see chapter 3). A dependency between strain hardening level (or hardness respectively) and high strain rates could not be observed [14].

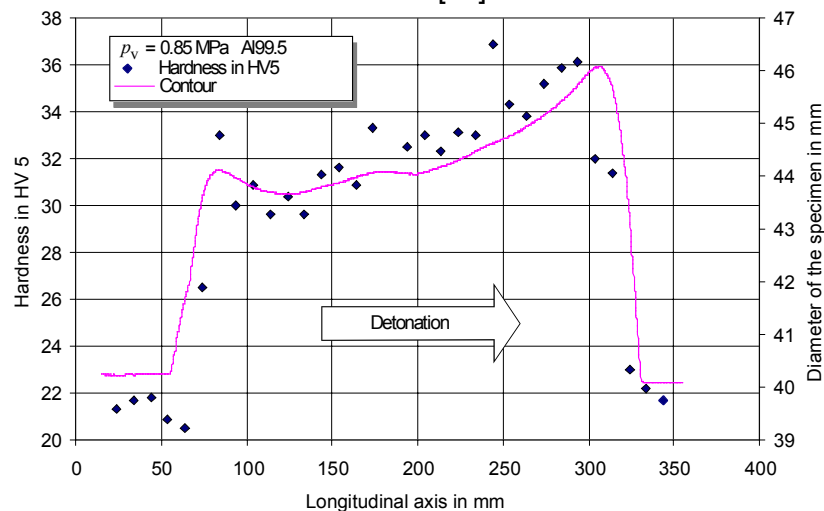


Figure 11: Left: hardness of the Al99.5 tubes versus rising diameters
Right: measurement of the lengthwise contour

6 Gas detonation experiments with die

For an industrial application it is necessary to use a die to realize reproducible workpiece contours. Furthermore, it is important to use more industrial-relevant materials like steel alloys and aluminum with higher strengths which were investigated here in a first approach.

6.1 Realized die construction

For the experiments a contour was used, which is a uniform enlargement of the tube diameter on a length of 300 mm. The cavity is changeable in its diameter by using changeable inserts (Figure 12). With this method it is possible to enlarge the diameter stepwise to find the biggest possible expansion without material failure. The workpiece is positioned between the upper and lower die and the axial sealing is realized on both sides by connexion nozzles. A possibility to generate a vacuum between cavity and workpiece was also realized to avoid negative effects caused by compressed air.

The shortness of the pressure shock in combination with the mass inertia of the tool system makes it possible to realize a forming of tubes with good calibration of details, e.g. small radii without high-performance presses, as they are needed in hydroforming processes [16].

Flexible tool systems were investigated during the experiments to enable an easy change of the dimensions of the workpiece. One example is using dies made of high-strength concrete. The manufacturing of these dies is similar to sandcast, using a turned polymer model. In this paper the experiments only included dies made of tool steel.

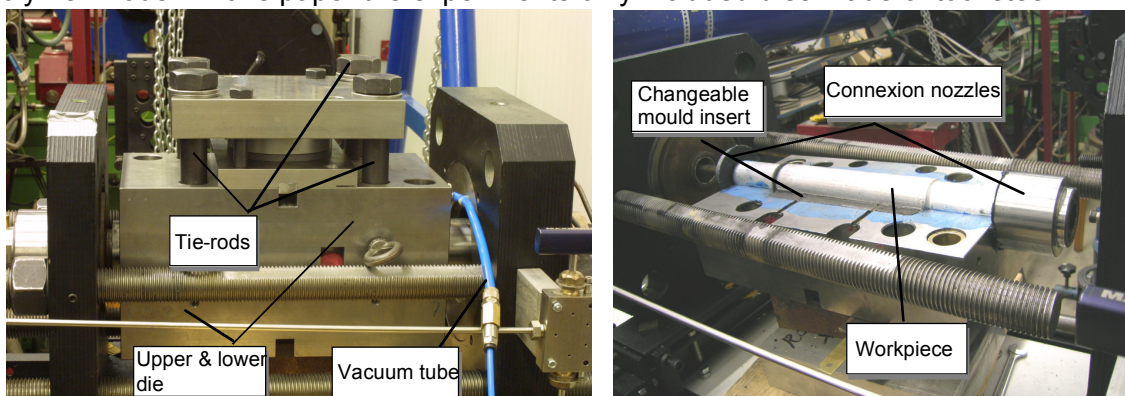


Figure 12: *Experimental set-up with die*

6.2 Experiments

As workpiece material the medium strength aluminum alloy AlMgSi1 (AA6082) was used. The material was precipitation-hardened at room temperature, resulting in a yield stress of $R_{p 0.2} = 110$ MPa and a tensile strength of $R_m = 205$ MPa. The theoretical elongation at break is 12 % [12]. In the static burst test without a die strain rates of approx. 8 % were achievable.

The experiments show that there is an according minimum pressure essential to realize an acceptable surface during forming operations in different diameters. This was demonstrated by a test made in an insert with a diameter of 47 mm. This is equivalent to 17.5 % tangential strain. At an initial pressure of 3 MPa no failure caused by crack formation was observed, but there were visible characteristic welding seams caused by the extrusion die. Using a higher initial pressure of the gas mixture of 3.5 MPa, the seams were not detectable any more. The high velocity impact of the tube walls levers the surface of the second workpiece. The surface details of the inserts can be found in the surface of the specimens. A strain rate influence of the material caused by the higher

initial pressure, and therefore a higher value of the expansion speed, is shown during the experiments, too (see chap. 3). An indication for this aspect is the noticeable diameter of 47 mm. In the static burst test without die only strains of approx. 8 % were achievable.

The behavior in the insert is shown in Figure 13. This contour measuring shows that a spring back effect can be located in the middle of the workpiece. The higher initial pressure of 3.5 MPa already shows a better calibration.

The maximum possible diameter up to now is 48 mm (Figure 13). This diameter was achieved at a test with an initial pressure of 4 MPa. This implies a tangential strain of 20 %. Here, it needs to be mentioned that there is only a small change in the total length of the workpiece. Before the experiments the length was defined by facing on a turning machine to be 358 mm. After the experiments the length was 357,5mm. So, the deformation is mainly realized by a reduction of the tube wall thickness. The static hydroforming test with the same die construction does not result in a successful workpiece with an insert with a diameter of 45 mm.

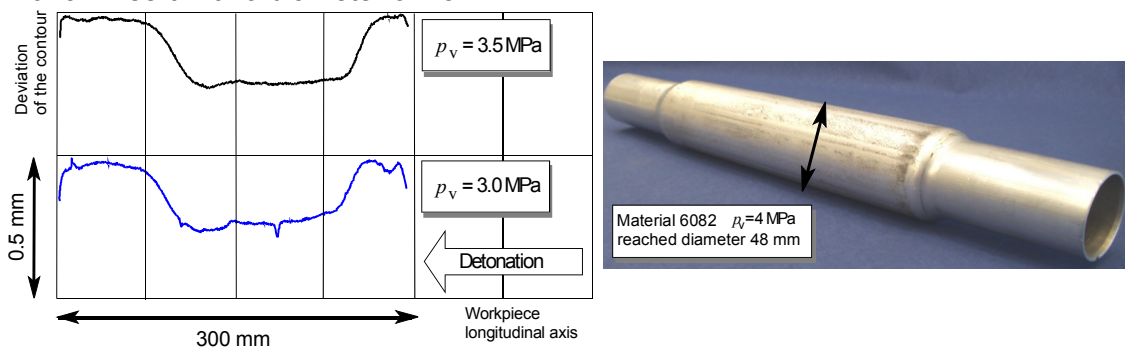


Figure 13: Left: moulding behavior; right: experiment with biggest diameter

To verify the influence of the special conditions in the process of gas detonation, reference experiments using hydroforming are done. A special hydroforming test tool was mounted on the 10MN press M+W BZE 1000-30.1.1 of the IUL.

The die has the same geometric features as in the gas detonation process. Thus, a direct comparison of the two processes is possible. During the experiments it was not possible to expand the AlMgSi1 tubes to a bigger diameter than 44 mm. The failure was caused by crack formation in the bulging of weak areas, mostly near the extrusion seams. It was possible to form Al99.5 workpieces calibrated at 60 MPa by an insert with a diameter of 47 mm.

7 Conclusion and Outlook

The experimental investigations of forming by gas detonation in combination with the numerical results, obtained by the developed simulation tool, have shown an enlargement of formability for the investigated types of aluminum. The accomplished material investigations confirmed this in general and identified the occurring high strain rates during the process as a major reason. Further investigations will focus on the detailed identification of process limits, adaptation of tool construction, application of different alloys, and complementary material analyses for a better understanding of this process combination. Thus, the long-term objective of a process design can be realized.

References

- [1] *Alshitz, V. I.; Indenbom V. L.:* Dynamic dragging of dislocations, Soviet Physics Uspekhi, Volume 18, Number 1, 1975
- [2] *Bartlmä, F.:* Gasdynamik der Verbrennung. Springer, Wien, Austria, 1975.
- [3] *Barrett, C.S.; Levenson, L.H.:* Formation of Etch Pits in Aluminium, Trans. Amer. Inst. Min. Met. Eng., Volume 137, S.112, 1940
- [4] *Bathe, K.-J.:* Finite Elemente Methoden, Springer-Verlag, 2. Auflage, 2002.
- [5] *Burden, R.; Snowden, L.; Hasegawa, K.; Newman, D.; Bauer, D.:* Elektromagnetisches Umformen. In: K. Siegert (Hrsg.), Tagungsband der Tagung „Neuere Entwicklungen in der Blechumformung“ 2000, 24. - 25. Mai 2000 in Fellbach, S. 331–354. Frankfurt, 2000.
- [6] *Czubayko, M.:* Korngrenzenbewegung in Aluminium und Zink, Aachen, RWTH, Diss., Shaker Verlag, 1998
- [7] *El-Magd, E.:* Fließkurvenermittlung im Hochgeschwindigkeitsbereich durch Versuch und numerische Simulation. Tagungsband zur Tagung „Werkstoffprüfung 1991“, 5. - 6. Dezember 1991, Bad Nauheim, S. 305-312.
- [8] *Esser, B.:* Die Zustandsgrößen im Stoßwellenkanal als Ergebnisse eines exakten Riemannlösers. Dissertation, RWTH Aachen, Germany, 1991.
- [9] *Gottstein, G., Shvindlerman, L.S.:* Grain boundary migration in metals: thermodynamics, kinetics, applications. Boca Raton, FL: CRC Press, 385 S., 1999
- [10] *Gottstein, G.:* Physik. Grundlagen der Materialkunde, Berlin Springer, 472 S., 2001
- [11] *Johnston W.G.; Gilman J.J.:* Dislocation Velocities, Dislocation Densities and Plastic Flow in Lithium Fluoride Crystals, Journal of Applied Physics, Volume 30, Number 2, S.129—144,1959
- [12] *Lehnert, W.:* Aluminium Taschenbuch Band 2. Aluminium-Verlag GmbH, Düsseldorf, 1996, p.96-100.
- [13] *Mattissen, D.:* In-situ Untersuchung des Einflusses der Tripelpunkte auf die Korngrenzenbewegung in Aluminium, Aachen, RWTH, Diss., Shaker Verlag, 2004
- [14] *Psyk, V.; Beerwald, C.; Homberg, W.; Kleiner, M.:* Electromagnetic Compression as Preforming Operation for Tubular Hydroforming Parts. Proceedings of the 1st International Conference on High Speed Forming (ICHSF) 2004, S. 171-180
- [15] *Roos, A.:* Fast-moving dislocations in high strain rate deformation, Groningen University Press, S. 29-58, 1999
- [16] *Thomas, W.:* Maschinenphysikalische Grundlagen patronenbetriebener trägheitsverriegelter Pressen zur Hochgeschwindigkeitsumformung, VDI-Verlag GmbH, Düsseldorf, p. 12-13, 1972
- [17] *Vohnout, V. J.:* A Hybrid Quasi-Static/Dynamic Process for Forming large Sheet Metal Parts From Aluminum Alloys. Ph.D. Dissertation of Vincent J. Ohio State University, Columbus, Ohio, USA, 1998.
- [18] *Vovk, V. T.:* Gasexplosion als "Werkzeug" in der Fertigungstechnik. Magdeburg, Univ., Habilitation, 1999.